

Symmetry breaking of the zero energy Landau level in bilayer graphene

Y. Zhao,¹ P. Cadden-Zimansky,^{1,2} Z. Jiang,³ and P. Kim¹

¹*Department of Physics, Columbia University New York, NY 10027*

²*National High Magnetic Field Laboratory, Tallahassee, FL 32310*

³*School of Physics, Georgia Institute of Technology, Atlanta, Georgia 30332, USA*

(Dated: May 7, 2019)

The quantum Hall effect near the charge neutrality point in bilayer graphene is investigated in high magnetic fields of up to 35 T using electronic transport measurements. In the high field regime, the eight-fold degeneracy in the zero energy Landau level is completely lifted, exhibiting new quantum Hall states corresponding filling factors $\nu = 0, 1, 2, \& 3$. Measurements of the activation energy gap in tilted magnetic fields suggest that the Landau level splitting at the newly formed $\nu = 1, 2, \& 3$ filling factors are independent of spin, consistent with the formation of a quantum Hall ferromagnet. In addition, measurements taken at the $\nu = 0$ charge neutral point show that, similar to single layer graphene, the bilayer becomes insulating at high fields.

PACS numbers: 73.63.-b, 65.80.+n, 73.22.-f

The unique chiral nature of the carrier dynamics in graphene results in a novel integer quantum Hall (QH) effect that distinguishes these atomically thin graphitic materials from conventional 2-dimensional systems [1, 2, 3]. The chiral nature of carriers in single layer graphene (SLG) and bilayer graphene (BLG) result in unevenly spaced Landau levels (LL) including a distinctive level located precisely at the particle-hole degenerate zero energy. While the energy spacing of SLG LLs scales as the square root of the LL index n and the square root of the field B , BLG levels have energies given by [4]

$$\epsilon_n^\pm = \pm \hbar \omega \sqrt{n(n-1)}, \quad (1)$$

where $\omega = eB/m$ is the cyclotron frequency with the BLG band mass $m \approx 0.05 m_e$, and n is a non-negative integer representing Landau orbit index in each layer. While the valley and spin degrees of freedom lead to a 4-fold degeneracy in graphene LLs, the additional orbital degeneracy for the $n = 0 \& 1$ indices in BLG result in a 8-fold degenerate, zero energy level that is unprecedented in LL physics [3, 4, 5].

At high fields, the decreasing radius of the cyclotron orbits gives rise to increasing electron-electron interactions which can perturb the degenerate LLs. Experiments on SLG have demonstrated this high-field symmetry breaking through the appearance of new QH states at the filling factor sequences $\nu = 0, \pm 1, \pm 4$ [6, 7, 8]. The precise nature of the field-dependent mechanisms that lift the degeneracies is still under experimental and theoretical debate [9, 10]. In particular, it has recently been observed that in SLG the $\nu = 0$ QH state becomes increasingly insulating at higher fields [11, 12]. Similar to SLG, the enhanced interactions under high magnetic field is expected to lift the 8-fold zero energy LL degeneracy in BLG. A number of theoretical predictions involving unusual collective excitations have been proposed to occur in this particle-hole symmetric LL as its degeneracy is broken [5, 13, 14, 15], but the experimental observation

of this broken symmetry is yet to be observed.

In this Letter we present transport measurements demonstrating the hierarchy of the splittings for the zero-energy LL in bilayer graphene as the external magnetic field is increased. Activation energy measurements of these splittings demonstrate energy spacing smaller than the bare electron-electron interaction energy and Zeeman energy. Tilted field measurements indicate that the degeneracy breaking at filling factors above the charge neutral point are independent of spin, consistent with the formation of a quantum Hall ferromagnet. While a quantum Hall plateau in the transverse resistance is observed at the charge neutral point, the longitudinal resistance at this point is seen to diverge to an insulating state with increasing field.

The graphene samples used in this work are deposited on SiO₂(300 nm)/Si substrates by mechanical exfoliation techniques from bulk single crystals [16]. The number of graphene layers are identified by optical contrast, cross-checked using Raman spectroscopy [17] and measurements of the high-field LL spectrum. Au/Cr electrodes for the graphene are fabricated by conventional electron beam lithography followed by metal evaporation. A gate voltage V_g is applied to the degenerately doped Si substrate to control the carrier density n_c according to the relation $n_c = C_g(V_g - V_D)/e$, where the areal gate capacitance is $C_g = 7.1 \times 10^{10} e/V \cdot \text{cm}^2$ and V_D is the gate voltage corresponding the charge neutrality point. The lower inset of Fig. 1a shows an optical microscope image of a typical BLG device used in this study. This device has a mobility as high as $\sim 1 \times 10^4 \text{ cm}^2/V \cdot \text{s}$ measured at the carrier density $n_h = 4 \times 10^{12} \text{ cm}^{-2}$. Since the electrodes of this device are configured in non-ideal Hall bar geometry, the magnetoresistance R_{xx} and Hall resistance R_{xy} were obtained following the van der Pauw method with symmetric (R_{xx}) and anti-symmetric (R_{xy}) averaging over data from positive and negative magnetic fields. The Hall conductivity σ_{xy} is then computed from R_{xx}

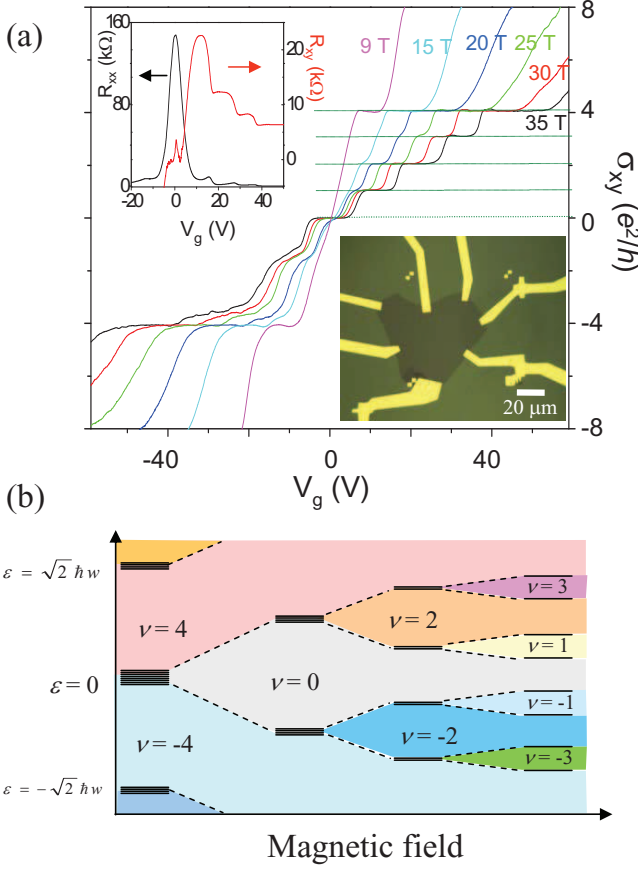


FIG. 1: (a) Hall conductivity σ_{xy} , as a function of gate voltage V_g at $T=1.4\text{K}$ at different magnetic fields: 9, 15, 20, 25, 30, and 35 T. Upper inset: R_{xx} (in black) and R_{xy} (in red) as V_g varies at $B=35\text{ T}$. Lower inset: optical microscope image of a BLG device used in this experiment. (b) Schematic of the zero energy LL hierarchy in bilayer graphene at high magnetic field.

and R_{xy} .

Fig. 1(a) shows R_{xx} and R_{xy} (upper inset) and σ_{xy} . As the back gate voltage alters the carrier density, QH plateaus in R_{xy} with corresponding zeros in R_{xx} are observed. Consequently, the calculated σ_{xy} shows well quantized plateau values at $\frac{1}{\nu} \frac{h}{e^2}$ with the integer filling factor ν . In the low magnetic field regime ($B < 10\text{ T}$), QH states corresponding to $\nu = \pm 4, \pm 8$ are present, as were previously seen in Ref. [3]. As B increases, however, new QH states emerge, as evidenced by additional QH plateaus at $\nu = 0$ & 2 and then $\nu = 1$ & 3 at higher fields.

In the high magnetic field regime, $B \gtrsim 20\text{ T}$, the new set of QH states demonstrate the full 8-fold degeneracy lifting in the zero energy LL. On close inspection of σ_{xy} in different magnetic fields, we can construct the hierarchical evolution of these new QH states. As the field increases from the low magnetic field regime, the $\nu = 0$ and 2 states start to develop at 15 T and are fully evolved

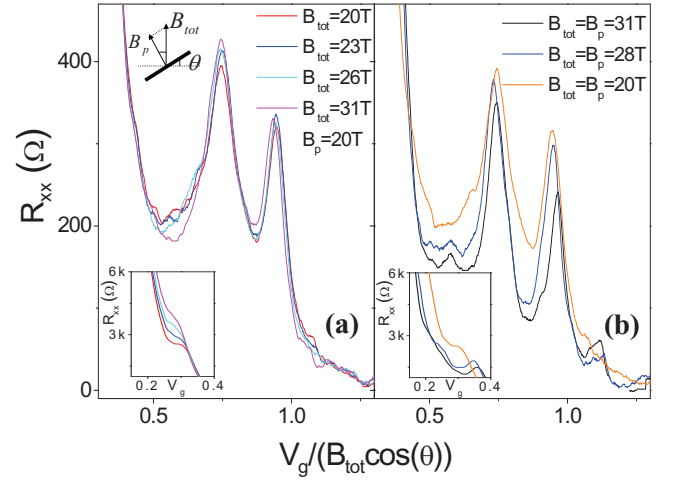


FIG. 2: (a) Magnetoresistance R_{xx} as a function of normalized back gate voltage $V_g/(B_{tot}\cos(\theta))$ around $\nu = 2$ and $\nu = 3$, at four different total magnetic fields with the same perpendicular field. Upper inset: Schematic diagram of tilted field; Lower inset: R_{xx} vs. $V_g/(B_{tot}\cos(\theta))$ at $\nu = 1$ state under the same condition as in the main figure. (b) R_{xx} as a function of normalized gate voltage with a zero tilting angle at different total fields, with the same scale of Fig2(a). Lower inset: R_{xx} vs. $V_g/(B_{tot}\cos(\theta))$ at $\nu = 1$ state. All data are taken at 1.5 K.

by 20 T; while the $\nu = 1$ and $\nu = 3$ states start to develop at 20 T and are fully evolved by 25 T. This hierarchical appearance of the new QH states is in accordance with the sequential symmetry breaking of the zero energy LL degeneracy as depicted in Fig. 1(b) and suggests that different symmetry-breaking processes are relevant as B increases.

Mechanisms for breaking the LL degeneracy include disorder, lattice strain, and charged impurities. The magnitude of the last of these can be estimated by assuming that the offset of the Dirac point gate voltage V_D from zero energy reflects a bilayer capacitively charged across the $d = 0.34\text{nm}$ layer spacing. From this model our measured $|V_D| \sim 2\text{ V}$ corresponds to a maximum charging energy of $\sim 2\text{ meV}$, small than, but of the same order as the high-field ($B \gtrsim 20\text{ T}$) bare Zeeman energy. In addition to the above mentioned graphene impurities, there are two field-dependent factors that can lead to the lifting of the eight degeneracies of this LL: Zeeman splitting of spin in magnetic field and electron-electron interactions that increase with field as the radius of the cyclotron orbits decrease. Zeeman splitting is given by $\Delta_z = g\mu_B B$, where μ_B is the Bohr magneton, and g is the gyromagnetic factor for the carriers in BLG. The Coulomb interactions between electrons are given by $e^2/\epsilon l_B$, where $\epsilon \sim 4$ is the dielectric constant for graphene and $l_B = \sqrt{\hbar/eB}$ is the magnetic length. In order to produce full 8-fold symmetry breaking, these mechanisms must lift not only the spin and valley degeneracies, but the $n = 0$ & 1 LL

orbital degeneracy. Barlas *et al.* have suggested that the exchange term from Coulomb interactions between electrons in these degenerate orbital states leads to a QH ferromagnetic state where the 8-fold symmetry is lifted by this exchange interaction. A Hund rule-like hierarchical symmetry breaking in the zero energy LL is predicted with this exchange-enhanced Zeeman splitting followed by the spin-independent valley and orbital splitting [5].

In order to test out this hierarchical degenerate lifting and the role of electron-electron interactions, we first note that sublattice or interlayer splittings that are associated solely with the Coulomb interactions between electrons localized in LL orbits should depend only on the normal magnetic field (B_{\perp}) but not the in-plane field (B_{\parallel}). Whereas spin-splitting includes a Zeeman component determined by the total field $B_{tot} = \sqrt{B_{\perp}^2 + B_{\parallel}^2}$. Experimentally, this idea can be tested out by measuring the samples in a series of tilted fields where we can examine the R_{xx} minima in different B_{\perp} and B_{\parallel} by tuning the tilting angle θ and B_{tot} . Fig. 2 displays the change of R_{xx} as a function of the gate voltage normalized by $B_{\perp} = B_{tot} \cos \theta$, in two different experimental conditions.

In Fig. 2(a), we first fix $B_p = 20$ T and then vary B_{\parallel} . For $\nu = 2, 3$ QH states, R_{xx}^{min} , the minima of R_{xx} corresponding to the QH zero magnetoresistance, display less than $\sim 10\%$ of variation, indicating no significant changes are induced by applying B_{\parallel} . For comparison, in Fig. 2(b), we show R_{xx} as a function of B_{\perp} with fixed $\theta = 0$, that is $B_{\parallel} = 0$ and $B_{\perp} = B_{tot}$. In this case R_{xx}^{min} for $\nu = 2$ and 3 increases by $\sim 40\%$ as B_{\perp} decreases from 31 T to 20 T, a factor of 4 larger change than the change of Fig. 2(a) where B_{tot} decreases from 31 T to 20 T while B_{\perp} was kept to 20 T. The fact that R_{xx}^{min} for $\nu = 2$ and 3 shows little to no dependence on the in-plane field strongly suggests that both these QH states are from non-spin origin and thus are due to the breaking of the valley or orbital degeneracy of the zero energy LL.

As for the $\nu = 1$ QH state, the experimental data of its tilted field dependence, shown in the insets of Fig. 2, displays an increasing R_{xx}^{min} with either a increasing in-plane field or a increasing normal field. While this evolution is consistent neither with an electron-electron or spin origin, it is likely that the increasing R_{xx}^{min} shown in the inset of Fig. 2(a) is due to the proximity of this filling factor to the increasingly insulating behavior of the bilayer at the charge neutrality point, discussed below. However, given the hierarchy of the degeneracy breaking, schematically shown in Fig. 1(b), the mechanism underlying the $\nu = 1$ breaking should be the same as that for $\nu = 3$, i.e. not from a spin origin, consistent with theoretical predications of the formation of a QH ferromagnet in BLG at high magnetic fields [5, 14].

To further understand the nature of the fully lifted LL degeneracy, we determine the energy of the LL splittings by measuring R_{xx}^{min} at different temperatures T . Fig. 3(a-

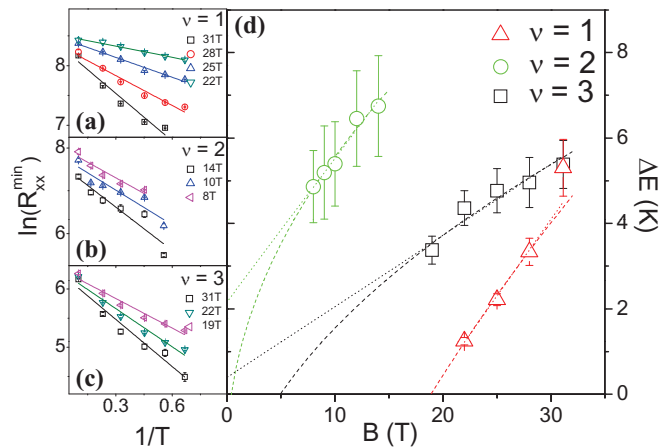


FIG. 3: (a) Arrhenius plots of R_{xx}^{min} 's as a function of $1/T$ at different fields for $\nu = 1$ state, the lines with respective colors are the linear fits to the data points. (b) Arrhenius plot for $\nu = 2$ state. (c) Arrhenius plot for $\nu = 3$ state. (d) Energy gap ΔE vs magnetic field B for different filling factors $\nu = 1$ (open triangle red), $\nu = 2$ (open circle green), $\nu = 3$ (open square black). The dotted lines are linear fits, whereas the dashed lines are square-root fits.

c) shows $\log R_{xx}^{min}$ versus $1/T$ for the $\nu = 1, 2, \& 3$ states. Since $R_{xx}^{min} \propto \exp[-(\Delta E - 2\Gamma)/2k_B T]$, where ΔE is the energy gap between two subsequent LLs and Γ is the LL energy broadening. The observed Arrhenius behavior in these plots allows us to estimate ΔE at different fields from the slope of the line fits. Fig. 3(d) displays the field dependence of the activation gap for $\nu = 1, 2, \& 3$. Generally, ΔE increases with increasing B as expected. It is also noted that at given B , $\Delta E_{\nu=2} > \Delta E_{\nu=3}, \Delta E_{\nu=1}$, indicating that the even ν states have larger energy than the odd ν QH states in accordance with the LL symmetry breaking hierarchy of Fig. 1(b). As for the field dependence, we find that a \sqrt{B} fit is better for $\nu = 2$ and $\nu = 3$ states. Attempts to fit the gap evolution linearly to B result in a positive y-axis intercept for the $\nu = 2$ and $\nu = 3$ gaps and a thus a non-physical negative LL broadening Γ . From the y-intercept of the \sqrt{B} dependence, we can extract a physically reasonable LL broadening of $\Gamma/k_B = 1.4$ and 3.7 K for the $\nu = 2$ and 3 states, respectively [18]. Although the apparent \sqrt{B} -dependence provides an independent confirmation of non-spin origin of the QH states $\nu = 1, 2, 3$, we note that the observed energy scale ΔE is still too small compared to the Coulomb energy or even the bare Zeeman energy. For $B = 15$ T, the Coulomb energy is 370 K and the Zeeman energy $E_z = 21$ K, both larger than $\Delta E_{\nu=2} = 8.6$ K at this field. It is possible that large amounts of disorder near the charge neutrality point of BLG are responsible for such a reduced transport gap.

We finally focus our attention on the $\nu = 0$ QH state. As with SLG, the presumed $\nu = 0$ splitting at the charge neutral point is not directly observable as a zero in R_{xx} .

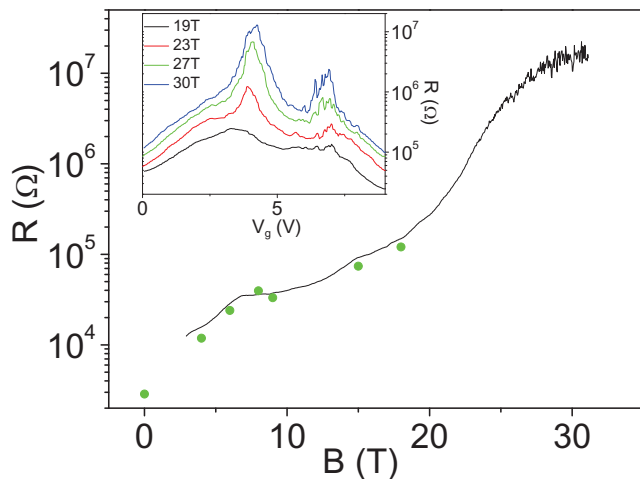


FIG. 4: Maximum resistance, measured in a two-probe constant voltage bias method, as a function of magnetic field, which is applied normally to the graphene plane, at a fixed gate voltage $V_g=4.1\text{V}$ around the charge neutrality point. The green dots are R_{xx}^{max} 's at $\nu = 0$ using a four-probe measurement. They are taken at lower magnetic fields ($B < 20\text{ T}$), and multiplied by a factor of 4 to match the 2 probe data. Upper left inset: Gatesweep of two-probe resistance at different fields: 19, 23, 27, and 29 T from bottom to top. All data are taken at 1.5K.

Rather, R_{xx} displays a maximum at this point, whose value increases with increasing B . In Fig. 4, we display our measurement of R_{xx} at the charge neutrality point in BLG. The measured resistance shows quasi-exponential growth as B increases, up to $\sim 10\text{ M}\Omega$ at 30 T. To avoid the self-heating of the graphene discussed in Ref. [12] and to measure resistances $> 10\text{ M}\Omega$ we employ a 2-probe AC measurement configuration with a constant voltage bias of $500\text{ }\mu\text{V}$, resulting in only $\sim 10\text{ fW}$ of heating at the highest fields. The contact resistance included in this measurement set-up is relatively small ($\sim 1\text{ K}\Omega$), but as an additional confirmation that it does not affect the behavior of the measured resistance, we cross-checked the 2-probe measurement using a conventional, current biased, 4-probe measurement at fields low enough that the resistance could be reliably measured with the voltage probes input to an amplifier with $10\text{ M}\Omega$ input impedance. The exponentially divergent R_{xx} behavior at high magnetic field is similar to analogous measurements that have been performed on SLG [11, 12], where a field-induced QH insulator has been proposed. We also note that the gate sweep (inset to Fig. 4) displays a growing number of local maximum in R_{xx} , presumably due to the inhomogeneous distribution of these insulating states at high magnetic field [19].

In conclusion, we have observed the full degeneracy lifting of the zero energy LL in bilayer graphene. Independent measurements of the longitudinal resistance zeros for the newly observed filling factors as a function of per-

pendicular field and temperature each indicate that the degeneracy lifting for the $\nu = 1, 2,$ & 3 splittings originate from electron-electron interactions. The field dependence of the longitudinal resistance at the $\nu = 0$ charge neutral point reveals insulating behavior similar in character to that of single layer graphene.

The authors thank D. Abanin, Y. Zhang, E. A. Henriksen, F. Ghahari, and Y. Barlas for helpful discussion, and thank S. T. Hannahs, E. C. Palm, and T. P. Murphy for their experimental assistance. This work is supported by DOE (No. DEFG02-05ER46215). A portion of this work was performed at the National High Magnetic Field Laboratory, which is supported by NSF Cooperative Agreement No. DMR-0654118, by the State of Florida, and by the DOE.

Note added.—During the preparation of this manuscript, we became aware of related work with a similar conclusion from Feldman *et al.* [20].

-
- [1] K. S. Novoselov *et al.*, Nature **438**, 197 (2005).
 - [2] Y. Zhang, Y. Tan, H. L. Stormer, and P. Kim, Nature **438**, 201 (2005).
 - [3] K. S. Novoselov *et al.*, Nature Phys. **2**, 177 (2006).
 - [4] Edward McCann and Vladimir I. Fal'ko, Phys. Rev. Lett. **96**, 086805 (2006).
 - [5] Yafis Barlas, R. Côté, K. Nomura, and A. H. MacDonald, Phys. Rev. Lett. **101**, 097601 (2008).
 - [6] Y. Zhang, Z. Jiang, J. P. Small, M. S. Purewal, Y. -W. Tan, M. Fazlollahi, J. D. Chudow, J. A. Jaszczak, H. L. Stormer, and P. Kim, Phys. Rev. Lett. **96**, 136806 (2006).
 - [7] Z. Jiang, Y. Zhang, H. L. Stormer, and P. Kim, Phys. Rev. Lett. **99**, 106802 (2007).
 - [8] A. J. M. Giesbers, L. A. Ponomarenko, K. S. Novoselov, A. K. Geim, M. I. Katsnelson, J. C. Maan, U. Zeitler, arXiv:0904.0948).
 - [9] Z. Jiang, Y. Zhang, Y. -W. Tan, H. L. Stormer, and P. Kim, Solid State Commun **143**, 14 (2007).
 - [10] K. Yang, Solid State Commun. **143**, 27 (2007).
 - [11] J. G. Checkelsky, L. Li, and N. P. Ong, Phys. Rev. Lett. **100**, 206801 (2008).
 - [12] J. G. Checkelsky, L. Li, and N. P. Ong, Phys. Rev. B **79**, 115434 (2009).
 - [13] K. Shizuya, Phys. Rev. B **79**, 165402 (2009).
 - [14] D. A. Abanin, S. A. Parameswaran, and S. L. Sondhi, arXiv:0904.0040.
 - [15] R. Nandkishore and L. Levitov, arXiv:0907:5395v1
 - [16] K. S. Novoselov, D. Jiang, T. Booth, V. V. Khotkevich, S. M. Morozov, and A. K. Geim, Proc. Natl. Acad. Sci. U.S.A. **102**, 10451 (2005).
 - [17] A.C. Ferrari, J. C. Meyer, V. Scardaci, C. Casiraghi, M. Lazzeri, F. Mauri, S. Piscanec, D. Jiang, K. S. Novoselov, S. Roth, A. K. Geim, Phys. Rev. Lett. **97**, 187401 (2006).
 - [18] For $\nu = 1$, the energy gap ΔE is too small to make a reliable fit for B dependence.
 - [19] S. Das Sarma, and Kun Yang, arXiv:0906.2209.
 - [20] B. Feldman, J. Martin, and A. Yacoby, arXiv:0907:5395v1.